Available online at www.sciencedirect.com
SCIENCE DIRECT®
International Journal of Solids and Structures 42 (2005) 591–604
INTERNATIONAL JOURNAL OF SOLIDS and STRUCTURES
www.elsevier.com/locate/ijsolstr

Nonlinear viscoelastic micromechanical analysis of fibre-reinforced polymer laminates with damage evolution

Yunfa Zhang, Zihui Xia *, Fernand Ellyin

Department of Mechanical Engineering, University of Alberta, Edmonton, Alta., Canada T6G 2G8

Received 14 April 2004
Available online 3 August 2004

Abstract

A micromechanical model of unidirectional fibre-reinforced polymer laminates under off-axis loading is analyzed using finite element method. A three-dimensional periodic unit cell is established with the matrix described by a nonlinear viscoelastic model and the fibre by an elastic one. Matrix cracking is modeled by smeared crack method which permits a crack description in terms of stress–strain relations and stiffness reduction in particular orientations. The micromechanical analysis features material nonlinearity, damage initiation and growth, and multiaxial loading. Numerical results reveal the local and global response of the laminate including the damage mechanism. The predictions are in good agreement with the test results performed on a similar composite system.

Keywords: Damage evolution; Fibre-reinforced polymer composite; Finite element analysis; Micromechanical analysis; Off-axis loading; Viscoelasticity

1. Introduction

The utilization of fibre-reinforced polymeric composites (FRPC) in various fields of application has progressed significantly over past decades. By using composite materials, designers are able to locate and orient the reinforcement to withstand the anticipated loads. However, in spite of the superior properties of composite materials, the use of composite materials in critical load bearing members is still limited. One of the main reasons for this limited application is the difficulty in reliable prediction of the behavior of composite materials. For example, the time- and temperature-dependent behavior of polymer matrices and the

* Corresponding author. Tel.: +1 780 4923870; fax: +1 780 4922200.
E-mail address: zihui.xia@ualberta.ca (Z. Xia).

0020-7683/$ - see front matter © 2004 Elsevier Ltd. All rights reserved.
doi:10.1016/j.ijsolstr.2004.06.021

mechanical degradation (damage) make the accurate prediction difficult, e.g. see Raghavan et al. (2001) and Kim et al. (2002), among others.

Most polymers are viscoelastic materials (some thermoplastic polymers may also be viscoelastic–viscoplastic). Although the fibres, such as E-glass fibre, behave elastically for most of their stress–strain range, composite laminates still exhibit viscoelasticity. For example, the analysis of Hashin (1966) showed that the viscoelastic effect in a unidirectional fibre composite is significant for axial shear, transverse shear and transverse uniaxial stress, for which the influence of matrix is dominant. The viscoelastic response of FRPC becomes even more pronounced under conditions of high temperature, sustained loading, and/or high stress level.

The presence of the epoxy matrix often has adverse effects on failure/damage properties, such as fracture toughness, creep rupture and fatigue life because of its brittleness. For example, matrix cracking could occur during manufacturing process or at relatively low applied loads. Damage (matrix cracking, interfacial debonding, etc.) can develop with increasing load, under cyclic loading, or even with increasing time under static loads. Therefore, it is important to model accurately the response of laminates with damage evolution.

Furthermore, an accurate composite analysis, especially with damage evolution, should consider the inherent length scales present in the composite. At least three scales are explicitly manifested in the composite laminates, viz. (a) the structural scale of the entire laminate, (b) the macroscopic scale of individual plies and (c) microstructural length scales of individual fibres, matrix, coatings or interfaces. In a typical FRPC, the diameter of each fibre is of the order of a few microns, and the thickness of the layers is of the order of 100 μm. Therefore, for damage initiation and evolution, a micromechanical analysis is required.

Micromechanical approach provides overall behavior of the composite through an analysis of a representative volume element (RVE) or a unit cell model (Aboudi, 1991; Nemat-Nasser and Hori, 1993). For composites with fibre arrays, a periodic structure is available and is generally referred to as a repeating unit cell (RUC). The advantage of this approach is not only in obtaining global properties of the composites but also various mechanisms such as damage initiation and propagation can be related to the constituents of composites (Xia et al., 2000; Ellyin et al., 2002).

Finite element method (FEM) has been extensively used to analyze a unit cell, to determine the mechanical response of composites (Adams and Crane, 1984; Bonora et al., 1994; Hollister and Kikuchi, 1992; Kim et al., 2002). In most cases, applications are limited to unidirectional laminate under uniaxial loading. A few investigators have also applied micromechanical analysis to the cross-ply laminates (laminates composed of 0° and 90° laminae) for which thermal residual stresses, viscoplastic or viscoelastic behaviors have been studied (Bigelow, 1993; Chen et al., 2001). Works on the analysis of unidirectional laminate under off-axis loading can be found, for example, in Aboudi (1991) and Zhu and Sun (2003). In addition, there have been a number of investigations in which damage modeling (matrix cracking and interface debonding) was incorporated into micromechanical analysis. In this type of approach the entire response of laminates under mechanical loading and the corresponding failure mechanisms can be simulated. However, as reviewed by Pagano and Yuan (2000), most of the micromechanical analysis of composites with damage modeling, has been confined to unidirectional laminate under uniaxial loading. A few investigations for cross-ply laminates have been reported e.g. see Xia et al. (2000), Ellyin et al. (2002) among others.

Two key requirements for an effective micromechanical analysis are: (a) an accurate constitutive model for the matrix material, and (b) a proper simulation of damage process (failure criterion and post-failure constitutive relation). In this paper, a micromechanical FEM model of a unidirectional FRPC laminate is presented which incorporates the combined effects of material nonlinearity, initiation of matrix cracking and damage evolution, as well as multiaxial loading. A three-dimensional unit cell is established with the matrix described by a nonlinear viscoelastic model and the fibre by an elastic one. The multiaxial loading

condition is specially treated using an iterative procedure since the analysis of a periodic unit cell requires application of proper periodic boundary conditions. A recently developed nonlinear viscoelastic constitutive model for the matrix is used to describe its time-dependent response under multiaxial loading. Matrix cracking is modeled by a smeared crack method which assumes the cracked solid to be continuum and permits a description in terms of stress–strain relations. The predicted results of a 45° off-axis loading are presented which include the local and global response of the laminate as well as damage evolution. These results are compared with the experimental data of a similar composite system, and the agreement is found to be good.

2. Micromechanical modeling of off-axis loading

The off-axis tensile loading applied to a unidirectional lamina can be decomposed into a set of multiaxial loading in the lamina coordinate system (corresponding to the principal material directions of a lamina), as shown in Fig. 1.

For 45° off-axis angle, we have,

$$\bar{\sigma}_{xx} = \bar{\sigma}_{yy} = \bar{\tau}_{xy} = \frac{1}{2}\bar{\sigma} \tag{1}$$

The response of a unidirectional laminate under the equivalent multiaxial loads will be analyzed here by a micromechanical method based on a unit cell. In a composite lamina the actual fibre distribution may not be entirely periodic across the cross-section. For the sake of simplicity, most micromechanical analyses of unidirectional laminates assume a periodic array of fibres for which a repeating unit cell can be isolated. The periodic fibre sequences commonly used are the square array and the hexagonal array (Sun and Vaidya, 1996; Kujawski et al., 1995). In this study, the square array of fibre distribution is assumed, resulting in a repeating unit cube containing one fibre. As shown in Fig. 2, the unit cell has the same fibre volume fraction as the unidirectional laminate and is meshed by eight node brick elements with 1536 elements and 1881 nodes.

A unified form of periodic boundary conditions for a unit cell or multiple cell models subjected to general multiaxial loads can be found in Xia et al. (2003a), which can easily be implemented in a FEM procedure. For the current problem, the boundary conditions are expressed as follows. Note that they constrain displacements on each pair of surfaces of the unit cell perpendicular to each coordinate axis, i.e.

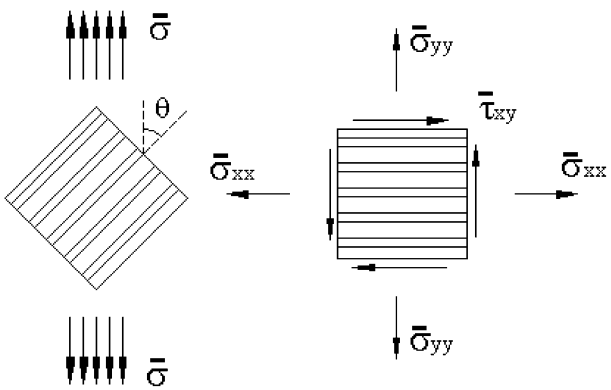

Fig. 1. A unidirectional laminate under off-axis tensile loading.

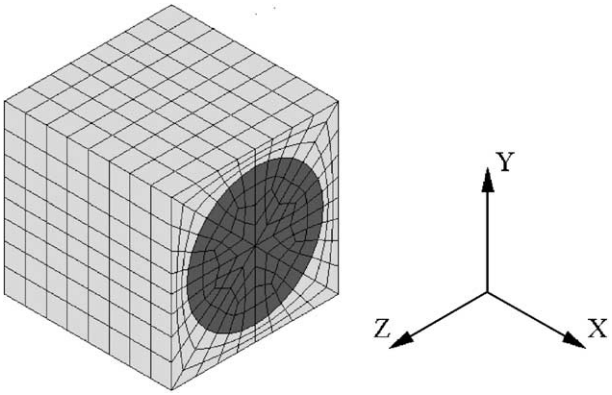

Fig. 2. A unit cell of unidirectional laminate.

On the planes perpendicular to X axis,

$$u(1,y,z)-u(0,y,z)=c_{11},\quad v(1,y,z)-v(0,y,z)=c_{12},\quad w(1,y,z)-w(0,y,z)=0 \tag{2}$$

On the planes perpendicular to Y axis,

$$u(x,1,z)-u(x,0,z)=c_{12},\quad v(x,1,z)-v(x,0,z)=c_{22},\quad w(x,1,z)-w(x,0,z)=0 \tag{3}$$

On the planes perpendicular to Z axis,

$$u(x,y,1)-u(x,y,0)=0,\quad v(x,y,1)-v(x,y,0)=0 \tag{4}$$

$$w(x,y,0)=0,\quad w(x,y,1)=\delta \tag{5}$$

And at the centre of the unit cell, $u=v=0$, to eliminate the rigid body motion. Note also that Eq. (5) indicates that in the Z direction, a generalized plane strain condition is adopted, which implies that the laminate is thick in the Z direction.

The global strain components can be taken as the average value over the unit cell, i.e.

$$\{\bar{\varepsilon}\}=\frac{1}{V}\int_V\{\varepsilon(x,y,z)\}\mathrm{d}V \tag{6}$$

Under the above boundary conditions, for a unit length cell, the nonzero global strain components are

$$\bar{\varepsilon}_{xx}=c_{11},\quad \bar{\varepsilon}_{yy}=c_{22},\quad \bar{\varepsilon}_{xy}=c_{12},\quad \text{and}\quad \bar{\varepsilon}_{zz}=\delta \tag{7}$$

Therefore, the global strain in the 45° direction is,

$$\bar{\varepsilon}=\frac{1}{2}(c_{11}+c_{22})+c_{12} \tag{8}$$

For each time step, Δt, the strain increment is given by

$$\Delta\bar{\varepsilon}=\dot{\varepsilon}\Delta t \tag{9}$$

where $\dot{\varepsilon}$ is the applied global strain rate. It is to be noted that in Eq. (1) the multiaxial loads are the global stress components applied to the unit cell model. An iterative procedure is required to ensure proper values of c_{11}, c_{22}, c_{12}, so that Eq. (1) is satisfied at each step. The iteration procedure is as follows:

(i) For each time step Δt, we have the trial values of c_{11}, c_{22}, c_{12}, which satisfy Eq. (8).
(ii) The solution with c_{11}, c_{22}, c_{12} gives the stress distribution in the unit cell, so the global stress components can be calculated from

$$\{\bar{\sigma}\} = \frac{1}{V}\int_V \{\sigma(x,y,z)\}\mathrm{d}V \tag{10}$$

where V is the volume of the unit cell.
(iii) Eq. (1) is checked and, if it is satisfied (within certain error limit), then next time step is proceeded. If not, new values of c_{11}, c_{22}, c_{12} are obtained and the steps (i)–(iii) are repeated. For a small time step, it could be assumed that the increments of c_{11}, c_{22}, c_{12} are proportional to the corresponding increment of average stress components, then the new values of c_{11}, c_{22}, c_{12} can be estimated from the average stresses, Eq. (10). Numerical calculation proved that by using this method the required values of c_{11}, c_{22}, c_{12} could be obtained through a few iterations.

3. Material model

The fibres behave elastically for most of their stress–strain range, so that they are modeled by the generalized Hooke's law. However, the epoxy matrix, like other thermoset polymers, has a highly nonlinear viscoelastic response. Therefore, an effective micro-mechanical analysis of fibre composites requires accurate constitutive relations for the matrix material. In this study, the epoxy polymer matrix is modeled by a nonlinear viscoelastic model (Xia et al., 2003b) and is summarized by the following expressions:

$$\{\dot{\varepsilon}_\mathrm{t}\} = \{\dot{\varepsilon}_\mathrm{e}\} + \{\dot{\varepsilon}_\mathrm{c}\} \tag{11}$$

$$\{\dot{\sigma}\} = E[A]^{-1}\{\dot{\varepsilon}_\mathrm{e}\} \tag{12}$$

In the above, $\{\dot{\varepsilon}_\mathrm{t}\}$, $\{\dot{\varepsilon}_\mathrm{e}\}$, $\{\dot{\varepsilon}_\mathrm{c}\}$, $\{\dot{\sigma}\}$ are the total strain-rate, elastic strain-rate, creep strain-rate, and stress-rate vectors (each contains six components, respectively). E is an elastic modulus which is assumed to be constant and $[A]$ is a matrix related to the value of Poisson's ratio, defined by

$$[A] = \begin{bmatrix} 1 & -\upsilon & -\upsilon & 0 & 0 & 0 \\ -\upsilon & 1 & -\upsilon & 0 & 0 & 0 \\ -\upsilon & -\upsilon & 1 & 0 & 0 & 0 \\ 0 & 0 & 0 & 1+\upsilon & 0 & 0 \\ 0 & 0 & 0 & 0 & 1+\upsilon & 0 \\ 0 & 0 & 0 & 0 & 0 & 1+\upsilon \end{bmatrix} \tag{13}$$

For a number of Kelvin (Voigt) elements connected in series, creep strain rate $\{\dot{\varepsilon}_\mathrm{c}\}$ is the sum of the strain-rate of each element $\{\dot{\varepsilon}_{\mathrm{c}i}\}$, i.e.

$$\{\dot{\varepsilon}_\mathrm{c}\} = \sum_{i=1}^{n}\left(\frac{[A]}{E_i\tau_i}\{\sigma\} - \frac{1}{\tau_i}\{\varepsilon_{\mathrm{c}i}\}\right) \tag{14}$$

In the above $\tau_i = \eta_i/E_i$ $(i = 1,2,\ldots,n)$ denotes the retardation time, E_i is the spring stiffness and η_i is the dashpot viscosity for the ith Kelvin (Voigt) element, respectively. Thus, the combination of Eqs. (11)–(14) provides a uniaxial representation consisting of one linear spring and several nonlinear Kelvin elements connected in series (Fig. 3). Based on experimental observations, the retardation time τ_i in Eq. (14) has a

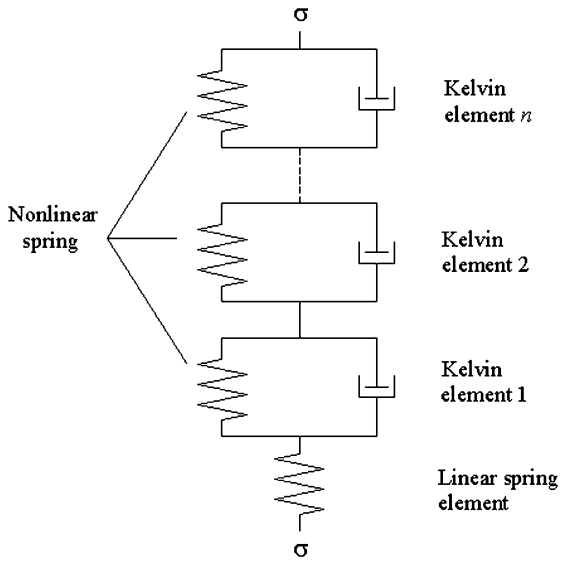

Fig. 3. A uniaxial visoelastic model represented by a finite series of Kelvin elements coupled with an elastic spring.

damped exponential character as in an exponential-type function. Its value determines the time duration after which contribution from the individual Kelvin element becomes negligible. Therefore, the number of the Kelvin elements adopted in the constitutive equation depends on the required time range. For simplicity, we introduce a time scale factor α, and assume that

$$\tau_i = (\alpha)^{i-1}\tau_1 \tag{15}$$

In this way all τ_i are related through the scale factor α. A time span of order of n would be covered, if n Kelvin elements were chosen and the value of α was taken to be 10.

The description of the nonlinear behavior in the current model was achieved by letting E_i's be functions of the current equivalent stress, σ_{eq}. Furthermore, a single function form for all E_i's is assumed, i.e.

$$E_i = E_1(\sigma_{eq}) \tag{16}$$

with

$$\sigma_{eq} = \frac{(R-1)I_1 + \sqrt{(R-1)^2 I_1^2 + 12RJ_2}}{2R} \tag{17}$$

where $I_1 = \sigma_1 + \sigma_2 + \sigma_3$ is the first invariant of the stress tensor, and $J_2 = S_{ij}S_{ij}/2$ is the second invariant of the deviatoric stress and R is the ratio of tensile to compressive 'yield stress'. Note that when $R = 1$, then Eq. (17) reduces to the von Mises equivalent stress, $\sigma_{eq} = \sqrt{3J_2}$. The multiaxial constitutive model of the thermosetting polymers includes a criterion which delineates loading and unloading behaviors. This will not be presented here and interested readers are encouraged to consult Xia et al. (2003b) and Hu (2002).

The values of constants (E, υ, α, τ_1, R) and the functional form of $E_1(\sigma_{eq})$ can be determined from uniaxial creep curves at different stress levels following a routine procedure which is described in the above mentioned references. The constants and functional form for an epoxy resin, Epon 826 with curing agent 9551, are listed in Table 1 (Xia et al., 2003b).

The composite system studied here is E-glass/epoxy matrix with fibre volume fraction of 52.5%. The fibre is modeled as an elastic material with Young's modulus $E = 72{,}500$ MPa and Poisson's ratio $v = 0.22$.

Table 1
Constants and function $E_1(\sigma_{eq})$

E (MPa)	v	α	τ_1	R
3400	0.42	10	6.116	1.15

$E_1(\sigma) = 1.055 \times 10^5 e^{-\frac{\sigma-22.764}{18.000}}$ MPa.

4. Modeling of matrix cracking

Upon increasing the applied load, microcracks will develop in the matrix. These cracks cause reduction in stiffness of the laminate. However, the laminate may continue to carry further load in spite of these cracks. In contrast to a single dominant crack in isotropic materials, the multiplicity of cracks in a laminate makes it difficult to deal with such cracks through the classical fracture mechanics approach. Instead, the so-called "smeared crack" approach (e.g., Rots, 1991) will be used. Here we briefly present the approach including numerical considerations.

4.1. Initiation of a crack

The first step is to determine the initiation of a crack using an appropriate damage criterion. Experimental investigation has indicated that the maximum principal strain theory is in good agreement with test data for matrix crack initiation in FRPCs (Hoover et al., 1997; Xia et al., 2000). Thus, at each step and at each matrix sampling point, the principal strains are computed, and a local (crack) coordinate system O-1-2-3 is established in which the three axes are along the directions of the three principal strains ($\varepsilon_1 \geqslant \varepsilon_2 \geqslant \varepsilon_3$, see Fig. 4).

The maximum principal strain damage criterion is then specified by

$$\varepsilon_1 \geqslant \varepsilon_{cr} \tag{18}$$

and when this condition is met, then a crack in the plane perpendicular to the direction of the ε_1 is deemed to have initiated.

4.2. Post-damage constitutive model

Once a crack is formed, it is assumed that it cannot transfer normal and shear stresses across the crack, i.e., σ_{11}, σ_{12} and $\sigma_{13} \to 0$. The subscript 1 denotes the Cartesian axis perpendicular to the plane of the crack

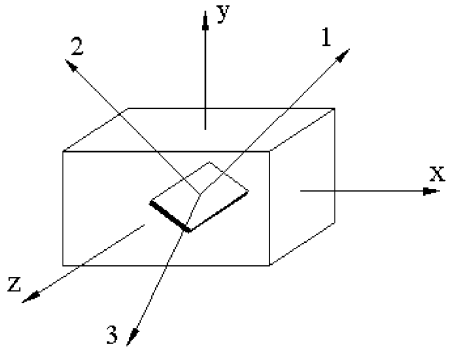

Fig. 4. Crack coordinate system.

while 2 and 3 are in the crack plane (see Fig. 4). However, the ability to transfer the other stress components is not affected by the crack formation. Let the stress and strain vectors in the local (crack) coordinate system be designated by,

$$\begin{aligned}\{\sigma\}^{\mathrm{cr}} &= [\sigma_1, \sigma_2, \sigma_3, \sigma_{12}, \sigma_{23}, \sigma_{31}]^{\mathrm{T}} \\ \{\varepsilon\}^{\mathrm{cr}} &= [\varepsilon_1, \varepsilon_2, \varepsilon_3, \gamma_{12}, \gamma_{23}, \gamma_{31}]^{\mathrm{T}}\end{aligned} \tag{19}$$

and stress and strain vectors in the global (O-x-y-z) coordinate system are,

$$\begin{aligned}\{\sigma\}^{\mathrm{gl}} &= \left[\sigma_{xx}, \sigma_{yy}, \sigma_{zz}, \sigma_{xy}, \sigma_{yz}, \sigma_{zx}\right]^{\mathrm{T}} \\ \{\varepsilon\}^{\mathrm{gl}} &= \left[\varepsilon_{xx}, \varepsilon_{yy}, \varepsilon_{zz}, \gamma_{xy}, \gamma_{yz}, \gamma_{zx}\right]^{\mathrm{T}}\end{aligned} \tag{20}$$

Thus, the post-damage constitutive model in the crack coordinate system is

$$\{\Delta\sigma\}^{\mathrm{cr}} = E_{\mathrm{t}}[D]\{\Delta\varepsilon\}^{\mathrm{cr}} - \chi[B]\{\sigma\}^{\mathrm{cr}} \tag{21}$$

or written in its full form

$$\begin{pmatrix} \Delta\sigma_1 \\ \Delta\sigma_2 \\ \Delta\sigma_3 \\ \Delta\sigma_{12} \\ \Delta\sigma_{23} \\ \Delta\sigma_{31} \end{pmatrix}^{\mathrm{cr}} = E_{\mathrm{t}} \begin{pmatrix} \beta Z_1 & 0 & 0 & 0 & 0 & 0 \\ 0 & Z_1 & Z_2 & 0 & 0 & 0 \\ 0 & Z_2 & Z_1 & 0 & 0 & 0 \\ 0 & 0 & 0 & \beta Z_3 & 0 & 0 \\ 0 & 0 & 0 & 0 & Z_3 & 0 \\ 0 & 0 & 0 & 0 & 0 & \beta Z_3 \end{pmatrix} \begin{pmatrix} \Delta\varepsilon_1 \\ \Delta\varepsilon_2 \\ \Delta\varepsilon_3 \\ \Delta\gamma_{12} \\ \Delta\gamma_{23} \\ \Delta\gamma_{31} \end{pmatrix}^{\mathrm{cr}} - \chi \begin{pmatrix} 1 & 0 & 0 & 0 & 0 & 0 \\ 0 & 0 & 0 & 0 & 0 & 0 \\ 0 & 0 & 0 & 0 & 0 & 0 \\ 0 & 0 & 0 & 1 & 0 & 0 \\ 0 & 0 & 0 & 0 & 0 & 0 \\ 0 & 0 & 0 & 0 & 0 & 1 \end{pmatrix} \begin{pmatrix} \sigma_1 \\ \sigma_2 \\ \sigma_3 \\ \sigma_{12} \\ \sigma_{23} \\ \sigma_{31} \end{pmatrix}^{\mathrm{cr}} \tag{22}$$

In the above,

$$Z_1 = \frac{1-\upsilon}{(1+\upsilon)(1-2\upsilon)}, \quad Z_2 = \frac{\upsilon}{(1+\upsilon)(1-2\upsilon)}, \quad Z_3 = \frac{1}{2(1+\upsilon)}, \tag{23}$$

E_{t} is the modulus of the epoxy under uniaxial tensile loading at the instant of damage, β is a small number which represents the loss of the stiffness in these three particular stress directions and the constant χ allows the three stress components to be reduced to near zero values in a sufficiently short time duration.

In Hu (2002), a series of uniaxial tensile tests on pure epoxy specimens at a strain rate of 10^{-4} s^{-1} gave the failure strain of 4.8%, therefore, the value of $\varepsilon_{\mathrm{cr}} = 4.8\%$ is used in this analysis. Also $E_{\mathrm{t}} = 284$ MPa is taken as the tangent modulus just before failure of the epoxy under the uniaxial tensile loading (Fig. 5).

The values of β and χ are taken to be 0.001 and 0.2, respectively in the current calculation. With such a choice of the values of the constants in Eq. (21), the above constitutive relation would reduce the stress components across the crack plane to a very small value in a short time (zero is the asymptotic limit). The matrix element then cannot carry loads in the corresponding direction; thus, simulating the damage process. Fig. 5 shows the response of a matrix element before and after damage. Also shown is the test result of epoxy specimens under uniaxial tensile loading at a strain rate of 10^{-4} s^{-1}. It can be seen that the response before failure is in good agreement with the test data. These values will be used in the following analysis for composite laminates.

It is to be noted that the formation of cracks would results in further anisotropy of an orthotropic composite laminate. However, this would not affect the application of periodic boundary conditions discussed earlier. In the current analysis, the laminate is seen as a periodical array of unit cells, each cell has the identical stress/strain field and the same cracking pattern.

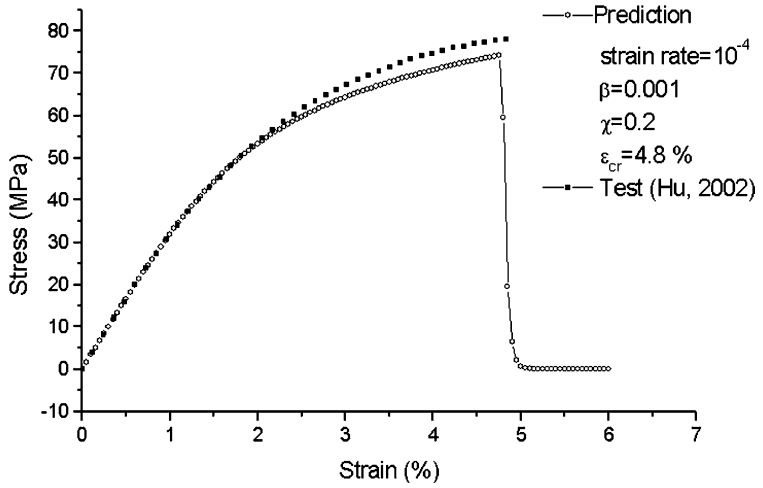

Fig. 5. The response of viscoelastic element before and after damage.

4.3. The stress and strain transformation from local to global coordinate system

The crack orientation in a 3D composite unit cell may vary at different locations; therefore, it would be convenient to have the post-damage relation transferred to the global coordinate system, where the FEA is carried out. Let the direction cosines of the principal strains $\varepsilon_i\,(i=1,2,3)$ be denoted by $(\ell_i\, m_i\, n_i)$. Therefore, the transformation matrix between the local and global coordinate systems can be written as,

$$[T]=\begin{bmatrix} \ell_1^2 & m_1^2 & n_1^2 & \ell_1 m_1 & m_1 n_1 & n_1 \ell_1 \\ \ell_2^2 & m_2^3 & n_2^2 & \ell_2 m_2 & m_2 n_2 & n_2 \ell_2 \\ \ell_3^2 & m_3^2 & n_3^2 & \ell_3 m_3 & m_3 n_3 & n_3 \ell_3 \\ 2\ell_1\ell_2 & 2m_1 m_2 & 2n_1 n_2 & \ell_1 m_2+\ell_2 m_1 & m_1 n_2+m_2 n_1 & n_1 \ell_2+n_2 \ell_1 \\ 2\ell_2\ell_3 & 2m_2 m_3 & 2n_2 n_3 & \ell_2 m_3+\ell_3 m_2 & m_2 n_3+m_3 n_2 & n_2 \ell_3+n_3 \ell_2 \\ 2\ell_3\ell_1 & 2m_3 m_1 & 2n_3 n_1 & \ell_3 m_1+\ell_1 m_3 & m_3 n_1+m_1 n_3 & n_3 \ell_1+n_1 \ell_3 \end{bmatrix} \tag{24}$$

The stress and strain transformation is given by

$$\{\Delta\varepsilon\}^{\mathrm{cr}}=[T]\{\Delta\varepsilon\}^{\mathrm{gl}},\quad \{\Delta\sigma\}^{\mathrm{cr}}=[T]^{-\mathrm{T}}\{\Delta\sigma\}^{\mathrm{gl}},\quad \{\sigma\}^{\mathrm{cr}}=[T]^{-\mathrm{T}}\{\sigma\}^{\mathrm{gl}} \tag{25}$$

Substituting Eq. (25) into Eq. (21), the post-damage constitutive equation in the global coordinate system is

$$\{\Delta\sigma\}^{\mathrm{gl}}=E_{\mathrm{t}}[D']\{\Delta\varepsilon\}^{\mathrm{gl}}-\chi[B']\{\sigma\}^{\mathrm{gl}} \tag{26}$$

with

$$\begin{aligned}[D'] &= [T]^{\mathrm{T}}[D][T] \\ [B'] &= [T]^{\mathrm{T}}[B][T]\end{aligned} \tag{27}$$

5. Results of 45° off-axis loading

The finite element code ADINA was used to conduct the numerical analysis. The viscoelastic constitutive relation of the resin matrix and the crack simulation procedure were implemented into the code through its user-defined subroutine. The displacement boundary conditions defined by Eqs. (2)–(5) are specified using constrain equations. The calculations were conducted on a SGI Origin 2000 computer system. A finer mesh of the unit cell was also used to verify the solution convergence of the analysis. The finer mesh has approximately doubled the number of elements and nodes as compared to the meshes shown in Fig. 2. It was found that there was no appreciable difference between the results of the finer mesh model and that shown in Fig. 2 with respect to global stress/strain relationship prior to damage, initiation of damage and propagation of the damaged zone.

5.1. Global response

Fig. 6 shows the predicted global stress/strain response of a 45° off-axis laminate and the comparison with the test results of Ellyin and Kujawski (1995) under a deformation controlled loading applied with a strain rate of 10^{-4} s^{-1}. The test specimens were made of "Scotchply 1003" prepregs of 3M Company. The fibre volume fraction was 52.5%. However, the properties of the epoxy matrix used in the "Scotchply 1003" prepreg were not available from the manufacturer, therefore, in the current calculation, the material constants for the Epon 826/curing agent 9551 have been used. It can be seen that the predicted trend is in good agreement with the test results. The predicted initial stiffness is 11.24 GPa, and the maximum load is 71.3 MPa, while the corresponding test results are 10.07 GPa and 83 MPa. One reason for the difference between the test data and the prediction is that the epoxy matrix in the prepreg was not the same as the Epon 826/Curing agent 9551 epoxy resin. As noted in Table 1, for the matrix, $E = 3400$ MPa, $v = 0.42$ and for the fibre, $E = 72\,500$ MPa, $v = 0.22$ were used in the current calculation. For the initial slope of the stress–strain curve of the composite (elastic modulus), both the elastic or the nonlinear viscoelastic analyses will predict very similar results. Using the aforementioned values in an elastic analysis one would obtain an elastic modulus of $E_{45} = 11.3$ GPa. However, if the elastic modulus of the epoxy matrix was taken

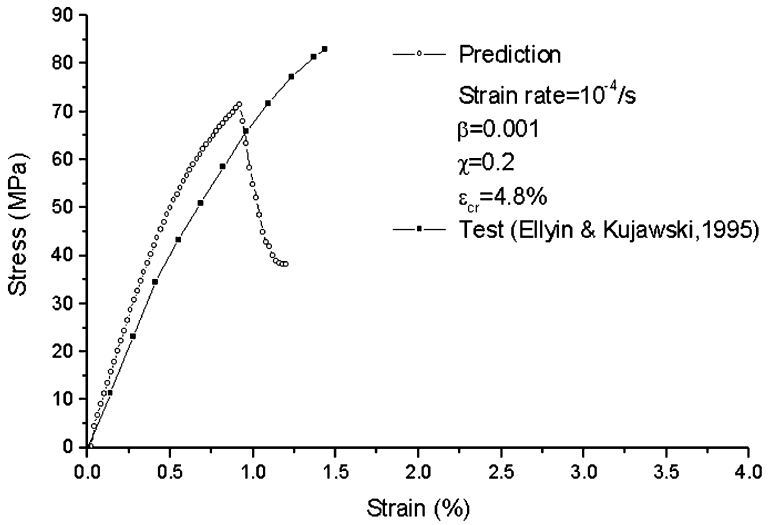

Fig. 6. Test data and predicted results of unidirectional laminate under 45° off-axis tensile loading.

as $E = 2950$ MPa and the other constants were kept the same, then one obtains, $E_{45} = 10.0$ GPa for the laminate, which is very close to the test value. Therefore, the discrepancy between the experimental and predicted value is most likely due to the overestimated elastic modulus of the epoxy polymer used in the prepreg sheets.

The effect of viscoelastic behavior of the matrix is manifested by the nonlinearity of the stress–strain curve, which is noticeable once the stress exceeds 40 MPa (about 0.5% strain). Since the damage has not yet occurred at this load level, therefore this nonlinearity is mainly caused by the viscoelasticity of the epoxy matrix.

5.2. Local response and damage evolution

The advantage of the current micromechanical method over the macromechanical modeling is that it provides a detailed stress/strain field in each constituent. It is the local stress/strain distribution which determines the damage initiation. Fig. 7 shows the distribution of the maximum principal strain in the unit cell at global strain of $\bar{\varepsilon} = 0.9\%$. Fig. 7(a) is an isometric 3D view and Fig. 7(b) is a front view at the fibre direction. As seen in Fig. 7(a), the distribution along the fibre direction (X-axis) is uniform. Also, it is clearly shown in Fig. 7(b) that the deformation is symmetric about the horizontal mid-plane. An examination of the distributions of other stress/strain components results in the same conclusion.

It can be seen that the maximum value of principal strain occurs in the matrix near the fibre/matrix interface and along the X-axis. Thus, upon further loading, there will be two symmetric 'narrow bands' of matrix cracking along the fibre direction.

The evolution of the damage zone (matrix cracking) can also be determined by the current analysis. Fig. 8 shows half of the unit cell. At an applied global strain of $\bar{\varepsilon} = 0.94\%$, the damage initiates in the form of

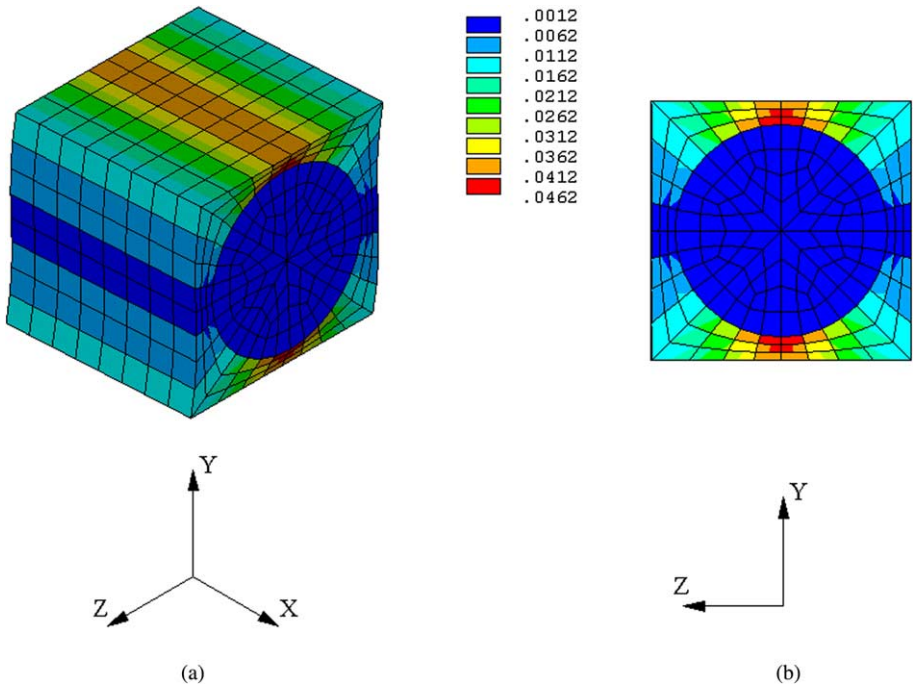

Fig. 7. First principal strain distribution in the unit cell: (a) isometric 3D view; (b) front 2D view.

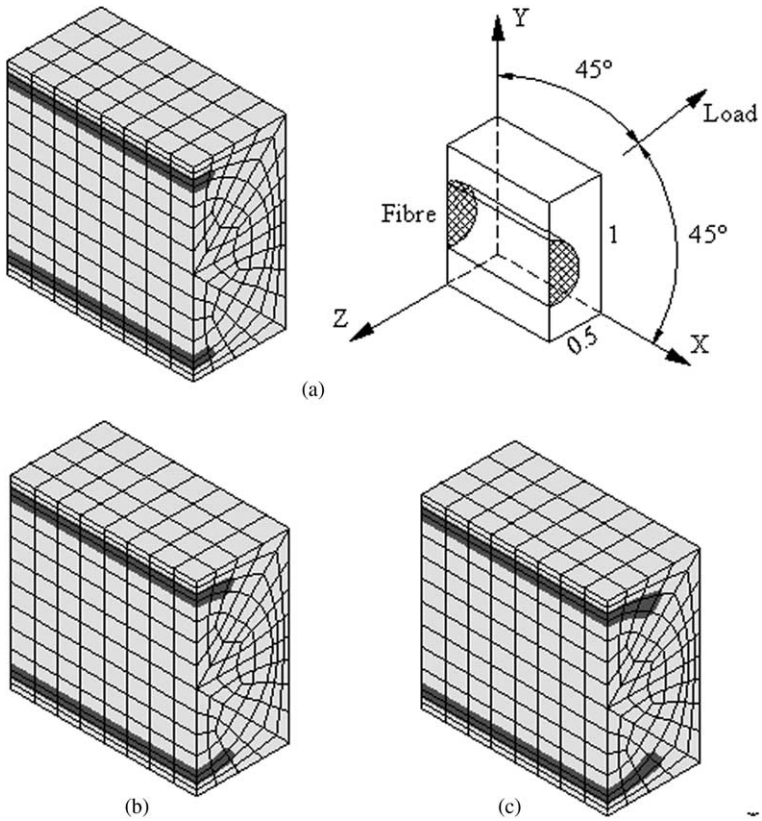

Fig. 8. Evolution of damaged zone: (a) $\bar{\varepsilon} = 0.94\%$; (b) $\bar{\varepsilon} = 1.0\%$; (c) $\bar{\varepsilon} = 1.2\%$.

two 'narrow bands' in the matrix near the interface along the fibre direction, Fig. 8(a). Upon further loading the bands expand around the circumference of the fibre. Note that the direction of global load is along the diagonal of the square cross-section. The predicted direction of the matrix cracking is in agreement with the test observations. In the tests of unidirectional coupon specimen under off-axis tensile loading, the cracks in the specimen and the final fracture of the specimen were along the fibre direction, see, e.g. El Kadi (1993).

6. Conclusions

The micromechanical FEM model of unidirectional FRPC laminates presented herein has successfully incorporated the combined effects of material nonlinearity and multiaxial loading. The damage initiation and growth, as well as global time-dependent response of a unidirectional fibre-reinforced laminate under off-axis loading are directly related to the properties of the constituents. The multiaxial loading condition is specifically treated using an iterative procedure which ensures a repeating unit cell undergoing proper periodic boundary conditions. The matrix cracking is modeled by the smeared crack method which allows for the loss of load transmission in particular orientations and permits a description of crack in terms of stress–strain relations. The periodic boundary conditions are implemented into a general purpose FEM code by specifying a number of constrain equations. The nonlinear viscoelastic behavior and the post-damage

material model are inserted into a FEM code by a user-defined subroutine. Thus, the current approach can easily be implemented for engineering applications.

Both global and local response of the unidirectional laminates under 45° off-axis loading are predicted, which are in good agreement with the experimental observations. Although only the results for 45° off-axis loading is presented herein, the approach is applicable in the analysis of unidirectional laminate under any off-axis angle. The approach can also be extended to analysis of angle-ply laminates under multiaxial loads, e.g. an elastic analysis for the angle-ply laminate can be found in Xia et al. (2003a).

Acknowledgments

The work presented here is part of a general investigation of the mechanical properties and damage prediction of composite laminates. The research is supported, in part, by the Natural Sciences and Engineering Research Council of Canada (NSERC) through grants to Z.X. and F.E.

References

Aboudi, J., 1991. Mechanics of Composite Materials, A Unified Micromechanical Approach. Elsevier Science Publishers, Amsterdam.

Adams, D.F., Crane, D.A., 1984. Finite element micromechanical analysis of a unidirectional composite including longitudinal shear loading. Computer and Structures 18, 1153–1165.

Bigelow, C.A., 1993. Thermal residual stresses in a silicon-carbide/titanium [0/90] laminate. Journal of Composites Technology and Research 15, 304–310.

Bonora, N., Costanzi, M., Newaz, G., Marchetti, M., 1994. Micro-damage effect on the overall response of long fibre/metal matrix composites. Composites 25, 575–582.

Chen, Y., Xia, Z., Ellyin, F., 2001. Evolution of residual stresses induced during curing processing using a viscoelastic micromechanical model. Journal of Composite Materials 35, 522–542.

El Kadi, H.A., 1993. Analysis and failure of laminated fibre reinforced composites. PhD thesis, Department of Mechanical Engineering, University of Alberta, Canada.

Ellyin, F., Kujawski, D., 1995. Tensile and fatigue behaviour of glass fibre/epoxy laminates. Construction and Building Materials 9, 425–430.

Ellyin, F., Xia, Z., Chen, Y., 2002. Viscoelastic micromechanical modeling of free edge and time effects in glass fibre/epoxy cross-ply laminates. Composites, Part A 33, 399–409.

Hashin, Z., 1966. Viscoelastic fibre reinforced materials. AIAA Journal 4, 1141–1147.

Hollister, S.J., Kikuchi, N., 1992. A comparison of homogenization and standard mechanics analysis for periodic porous composites. Computational Mechanics 10, 73–95.

Hoover, J.W., Kujawski, D., Ellyin, F., 1997. Transverse cracking of symmetric and unsymmetric glass-fibre/epoxy-resin laminates. Composites Science and Technology 57, 1513–1526.

Hu, Y., 2002. Multiaxial behavior and viscoelastic constitutive modeling of epoxy polymers. PhD thesis, Department of Mechanical Engineering, University of Alberta, Canada.

Kim, S.J., Lee, C.S., Yeo, H.J., 2002. Direct numerical simulation of composite structures. Journal of Composite Materials 36, 2765–2785.

Kujawski, D., Xia, Z., Ellyin, F., 1995. Morphology/loading direction coupling on the transverse behaviour of composites. In: Pyrz, R. (Ed.), IUTAM Symposium on Microstructure–Property Interactions in Composite Materials. Kluwer Academic Publishers, Netherlands, pp. 203–213.

Nemat-Nasser, S., Hori, M., 1993. Micromechanics: Overall Properties of Heterogeneous Materials. Elsevier Science Publishers, Amsterdam.

Pagano, N.J., Yuan, F.G., 2000. The significance of effective modulus theory (homogenization) in composite laminate mechanics. Composites Science and Technology 60, 2471–2488.

Raghavan, P., Moorthy, S., Ghosh, S., Pagano, N.J., 2001. Revisiting the composite laminate problem with an adaptive multi-level computational model. Composites Sciences and Technology 61, 1017–1040.

Rots, J.G., 1991. Smeared and discrete representations of localized fracture. International Journal of Fracture 51, 45–59.

Sun, C.T., Vaidya, R.S., 1996. Prediction of composite properties from a representative volume element. Composites Science and Technology 56, 171–179.

Xia, Z., Chen, Y., Ellyin, F., 2000. A meso/micro-mechanical model for damage progression in glass-fibre/epoxy cross-ply laminates by finite-element analysis. Composites Science and Technology 60, 1171–1179.

Xia, Z., Zhang, Y., Ellyin, F., 2003a. A unified periodical boundary conditions for representative volume elements of composites and applications. International Journal of Solids and Structures 40, 1907–1921.

Xia, Z., Hu, Y., Ellyin, F., 2003b. Deformation behavior of an epoxy resin subject to multiaxial loadings. Part II: Constitutive modeling and predictions. Polymer Engineering and Science 43, 734–748.

Zhu, C., Sun, C.T., 2003. Micromechanical modeling of fibre composites under off-axis loading. Journal of Thermoplastic Composite Materials 16, 333–344.